

A unified approach for representing fretting and damage at the edges of incomplete and receding contacts

D.A. Hills¹, R. Ramesh^{1,*}, R. M. N. Fleury¹, and K. Parel¹

¹Department of Engineering Science, University of Oxford, Parks Road, Oxford

OX1 3PJ, United Kingdom

*rangarajan.ramesh@eng.ox.ac.uk

Abstract

This paper attempts to unify the analysis of fretting and damage at the edges of different classes of contact. Specifically edge asymptotes may be applied, in the same form, to both incomplete and to receding contacts. The benefit of this approach is that experiments carried out on incomplete contacts may be used to predict the life of a wide range of incomplete contact geometries, and also of receding contacts.

Keywords: Contacts, Incomplete Contacts, Asymptotes, Fretting

1 Introduction

The nucleation of fatigue cracks under conditions of fretting remains something which is not fully understood and, indeed, the micromechanics of the process are likely to remain elusive and also to vary from alloy to alloy. So, although there has, and continues to be, a lot of interest in modelling this process, usually through some form of critical plane analysis, we advocate a wholly different approach. The basic idea is that a (small) family of local solutions, centred on the edge of the contact, and which implicitly includes a lot of information about the local stress field, including both the stress gradient and polar variation of stress components, is fitted to the edge of the contact. As will be seen, these solutions fully describe the contact tractions, extent of

slip, slip displacement, and all other relevant information which might have a bearing on crack nucleation. It follows that, if laboratory tests are carried out in which the history of these local solutions is well specified, both the threshold for infinite life (and, in the case of finite life, the number of cycles taken to nucleate a crack), of a prototype suffering the same history of local solutions must have exactly the same life; the micromechanics of what goes on within the domain of that local solution need not concern us.

Before we can begin the analysis we need to carry out a taxonomy of all possible classes of contact which might be found in any prototype, and, in Figure 1.1 we show, in idealised form, the four basic forms of behaviour which might be experienced. It is assumed that the components experiencing fretting are made from metals or alloys, and that the overall loads are such as to maintain an elastic macroscopic stress state in the material: the deformation of the components is therefore small and conventional linear elasticity with no significant rotation of material elements applies. The state of stress varies with a radial coordinate from the contact edge, s , in a characteristic way. First, Figure 1.1a shows an incomplete contact (in fact a cylinder pressed onto a flat, but other problems falling into this class include a shallow wedge or, more practically, the dovetail root of a fan blade root), where both bodies may, in the neighbourhood of contact, be idealised by a half plane (or half-space in three dimensions). When half-plane theory is employed we may show from the properties of singular integral equations usually employed to solve contact problems [1] that the contact pressure, $p(s)$, must be locally square root bounded, ie. $p(s) \propto \sqrt{s}$. A similar kind of contact which is incomplete but which may not be modelled using half plane theory, such as the pin in an almost conforming hole, (a more practical case of a problem of this class would be the edge of a turbine blade firtree root in a gas turbine) is shown in Figure 1.1b. It is *still* the case that locally the contact edge still behaves as a half plane, and hence the contact pressure still decays in a square root bounded manner.

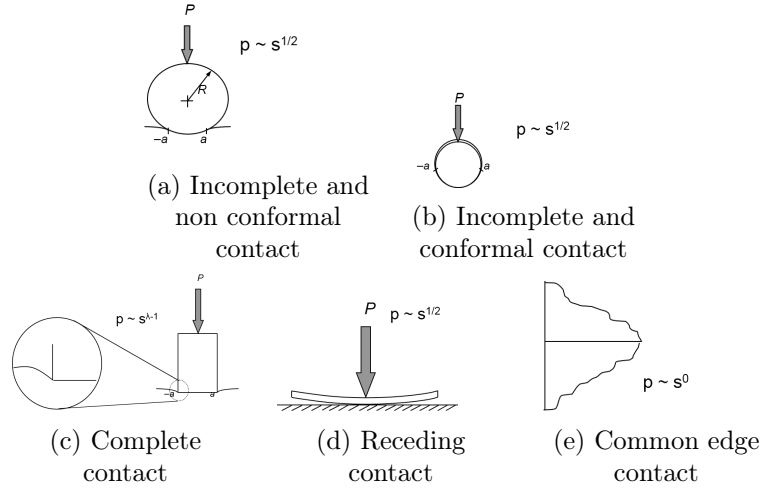


Figure 1.1: Fundamental classification of contacts

We turn, now, to a complete contact such as the one depicted in Figure 1.1c in which an elastic block is pressed into an elastically similar half-plane (a contact occurring in a gas turbine of this class is the spline joint between split shafts). Here, there are a number of possibilities depending on the contact edge behaviour and whether the contact is locally stuck [2, 3] but, in every case, the contact pressure will vary as $p(s) \propto s^{\lambda-1}$, where λ is an eigenvalue of a characteristic equation, parametrically dependent on the local contact angle and coefficient of friction, but almost invariably $0 < \lambda < 1$, so that the contact pressure, moving towards the contact edge, displays a power order singular characteristic. Figure 1.1d depicts a receding contact. The most commonly occurring cases are in bolted joints, where the very localised contact pressure beneath the bolt causes the interface to separate away from the point of application of the applied force. These will be described in more detail in a later section, but we note, here, that the contacting surfaces at the point of separation have a common tangent, and so locally these are again very similar in behaviour to an incomplete, half-plane contact, and hence the contact pressure displays square root bounded characteristics. Lastly, in Figure 1.1e we show, in idealised form, the edge of a contact formed by two bodies whose edges are aligned, so that the location of the contact edge is defined by both bodies simultaneously. Contacts with a common edge still have a local stress distribution with a characteristic local polar form [4, 5], and the contact pressure is finite and non zero, i.e. $p(s) \propto s^0$. So, it may be seen that complete contacts and those having a common edge exhibit a different edge characteristic from incomplete and receding contacts. We will, in the rest of this paper, restrict ourselves to consideration of contacts displaying square root bounded contact edge behaviour,

and show how problems of these classes may be treated uniformly if only the contact edge behaviour, including the presence of local slip, are needed. This is invariably the case when fretting fatigue arises.

2 Basic Solutions

The best way to describe contact edge behaviour is to assume, for the time being, that the coefficient of friction, f , is sufficient high to inhibit all slip. Figure 2 shows a generic incomplete contact (which need not be Hertzian). If the contact half-width is a the symmetric shear traction, $q(x)$ induced by the application of a shear force Q is given by

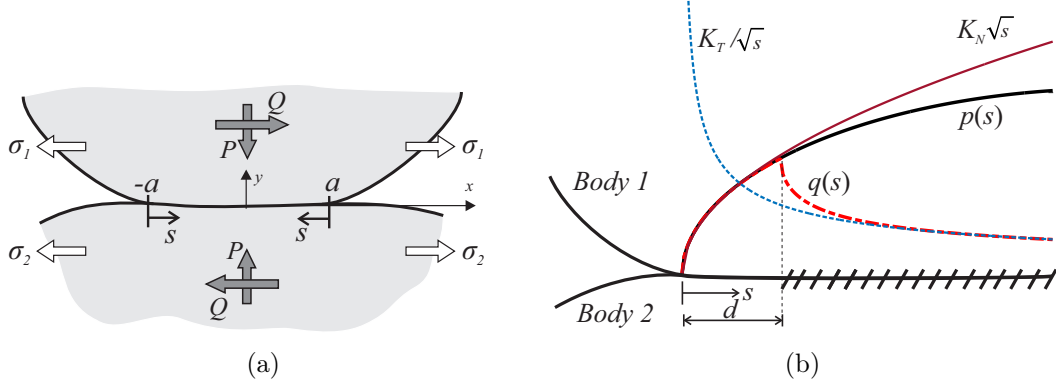


Figure 2.1: (a) Incomplete fretting problem under normal, shear and bulk tension loading, (b) Contact tractions and edge asymptotes

$$q(x) = \frac{Q}{\pi\sqrt{a^2 - x^2}}. \quad (2.1)$$

It is rare for contacts to suffer only a net force, and, in most cases, tensions parallel with the free surfaces will be present. If that in the upper body is σ_1 and that in the lower body is σ_2 an antisymmetric shear traction distribution is induced given by

$$q(x) = -\frac{\sigma_0 x}{4\sqrt{a^2 - x^2}}, \quad (2.2)$$

where $\sigma_0 = \sigma_1 - \sigma_2$. Notice that these results are independent of the geometry of the indenter, and that, if we move the origin to a local one positioned at either edge of the contact, positive inwards, Figure 2.1a, and then expand these expressions by the binomial theorem and take the dominant term, we see that the local shear traction is given by

$$q(s) = \frac{K_T}{\sqrt{s}}, \quad (2.3)$$

where

$$K_T = \pm \frac{Q}{\pi\sqrt{2a}} + \frac{\sigma_0}{4} \sqrt{\frac{a}{2}}, \quad (2.4)$$

and the +ve sign is taken for the left hand edge ($x \rightarrow a^+$) and the -ve sign is taken for the right hand edge ($s \rightarrow a^-$). These expressions display the magnitude of the shear stress singularity at each edge of the contact and show that the application of a differential surface tension is additive to the effects of a shear force at one end of the contact but is subtractive from it at the other. We turn, now, to the solution for the contact pressure. For incomplete contacts this may always be written in the form

$$p(s) = K_N \sqrt{s}, \quad (2.5)$$

and so we define the multiplier $K_N [FL^{-5/2}]$ by

$$K_N = \lim_{s \rightarrow 0} \frac{p(s)}{\sqrt{s}}. \quad (2.6)$$

For simple geometries this may be evaluated analytically so that, for example, for a Hertzian contact

$$K_N = \frac{P}{\pi} \sqrt{\frac{8}{a^3}}, \quad (2.7)$$

and for complex profiles where the finite element method is used the value may be abstracted by conventional numerical procedures¹. Once the values of K_N, K_T are known, giving the fully adhered contact edge response, the effect of friction may easily be found. This is, of course, loading trajectory dependent and so, here, we will consider the case where first the normal load is applied, and subsequently held constant. By using the Ciavarella-Jäger theorem [7, 8] the corrective solution for the shear traction may be found [9, 10], and the size of the slip zone for a monotonically increasing set of loads producing advancing slip, determined. The steady state (reversing) slip zone size under reversing loading is also given. This has the result, for the *steady state*, of a slip zone of length d , given by

¹This is related, we believe, to the quantity, I^s , introduced by Montebello [6], which he refers to as the ‘velocity field’, and we believe is defined by the relationship $\frac{\partial p(x,a)}{\partial a} = \frac{I^s}{\sqrt{a-x}}$. It may easily be shown to be related to the quantity $K_N = 2I^s$.

$$fd = \frac{\Delta K_T}{K_N}, \quad (2.8)$$

where ΔK_T is the range of shear stress intensity, and the shear traction is given by

$$q(s) = fK_N\sqrt{s} = \frac{K_T}{d}\sqrt{s} \quad 0 < s < d \quad (2.9)$$

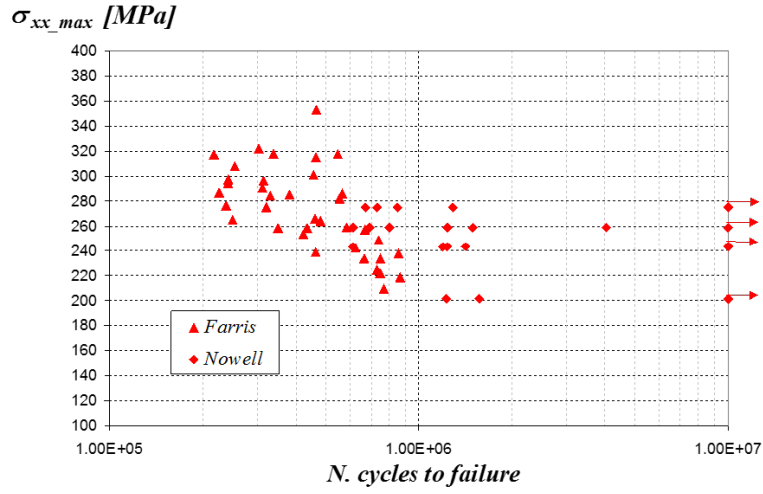
$$q(s) = \frac{K_T}{d}(\sqrt{s} - \sqrt{s-d}) \quad d < s, \quad (2.10)$$

and both the full stick tractions, together with those in the presence of slip are shown, for a representative case, in Figure 2.1b. Recent work [11] has investigated the effects of different mixes of tension and shear force more fully, and also looked at the effects of truncating what is, in effect, a series expansion of the tractions to a single term, has on accuracy.

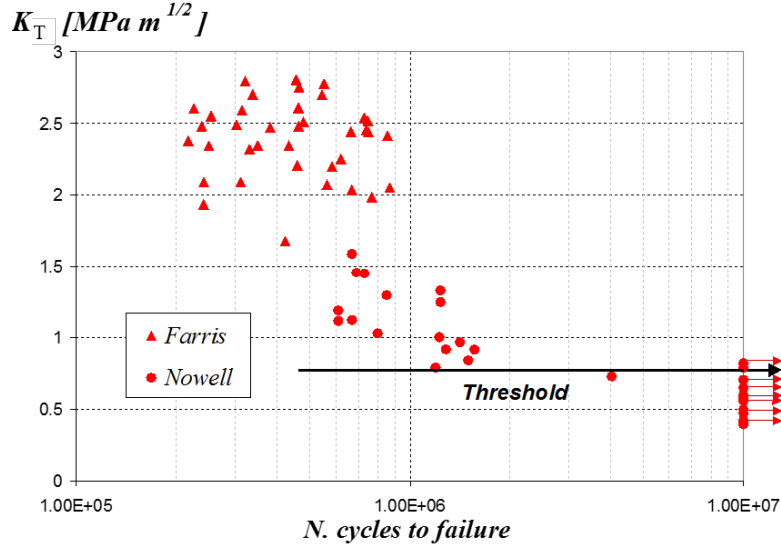
3 Experimental Evidence

In the vast majority of fretting fatigue tests carried out using incomplete contacts published so far, the normal load is held constant so that the analysis described above applies in full [12, 13]. As the coefficient of friction is also taken to be a material property, it follows that the only two parameters which govern the traction distribution, extent of slip (in the steady state), range of slip displacement and, indeed, the whole stress field in the hinterland [14], are the parameters $K_N, \Delta K_T$. Furthermore, the quantity K_N is held constant during tests and so is likely to have only a secondary effect on fatigue strength, although we should note that it does control the extent of the slip region. We expect it to be the range of shear tractions, encapsulated in ΔK_T , which has the primary effect. In Figure 3.1, to illustrate the validity of this assertion, we plot the number of cycles to failure against this quantity. Also included in the figure is a conventional ‘S-N curve’ plot, where ‘S’ is taken as that stress at the surface at the point of crack nucleation. The results shown are for a commonly investigated 4% copper aluminium alloy, and include those found by Nowell [15] and those independently found by Szolwinski [16] using a different test apparatus. It is clear that the S-N curve is completely unhelpful, and shows that omitting the size effect invalidates the approach, whereas using the generalised stress intensity for shear ($\Delta K_T[FL^{-3/2}]$) implicitly includes stress gradient information, and this is very much cleaner. The threshold value is particularly well defined. The finite life data remains spread, but much less so than in the S-N plot, and we must bear in mind; (a) that

N is the number of cycles to failure, whereas the asymptotic field derived above encapsulates only the nucleation process and (b) a limitation of the approach is that the developing crack grows away from the origin of the asymptote and therefore inexorably into a region where the asymptotic form has decreasing dominance. This we may contrast with the crack tip stress intensity solution which remains, of course, attached to the propagating crack tip and therefore maintains its precision. A further example of when asymptotics were used effectively to analyse sharp edge contacts may be found in Bertini and Santus [17].



(a) Cycles to failure against the stress at the surface point of crack nucleation (trailing edge)



(b) Cycles to failure against the generalised stress intensity factor ΔK_T

Figure 3.1: Experimental fretting fatigue date: number of cycles to failure as a function of two possible nucleation-controlling variables [15, 16, 14]

4 Slight rounding; local half-plane behaviour

Encouraged by the effectiveness of the correlation of fretting fatigue data, we have gone on to look at a number of extensions to the basic idea. In the first of these, we examine what happens in a problem where, although the behaviour in the hinterland of the contact edge is clearly anything but half-plane in character, the contact edge itself retains half-plane characteristics so that the asymptotic forms derived remain valid. To illustrate this point we look not at the conformal contact shown in the introduction, but a local solution intended to represent the effects of a very small amount of rounding on what is, otherwise, a complete contact, Figure 4.1a.

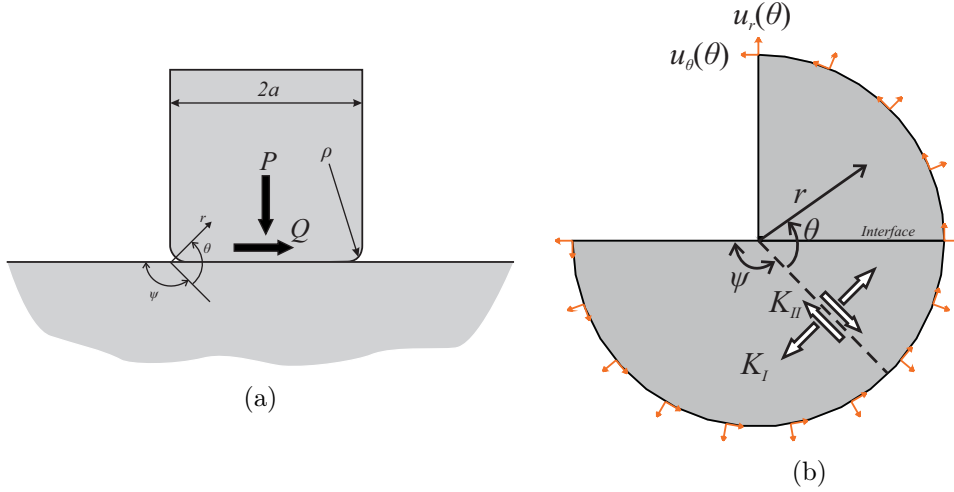


Figure 4.1: (a) Complete contact with small rounding, (b) Finite Element three quarter plane model

An earlier form of the solution used the formulation for a finite punch having a flat face but with rounded edges, and took the limit when the flat length became infinitely long [18]. This was based on a half-plane idealisation and led to the contact pressure remote from the edges decaying in a square root fashion. This form of the solution is therefore appropriate only when the contact-defining body is rigid and the half-plane incompressible, whereas a solution is needed where the bodies are elastically similar and, remote from the edges, the state of stress is represented faithfully by a Williams-type solution specialised to a three-quarter-plane (if the punch has corners which are right angles). To do this a finite element model of a three quarter plane with a very small edge radius (1/100 of the radius of the model, Figure 4.1b) was set up. The boundary was loaded by imposing displacements, and were exerted in the form implied by the Williams solution, so that the ‘material beyond the model’ itself appeared to be a three quarter plane, and the state of stress looking inwards towards the corner

continued to behave in this fashion until the observation point approached the corner. At very small distances the state of stress now looks to be that observed near the edge of a bounded contact, i.e. it has a form, near the edge, which is square root bounded in character. If the radius of the contact edge is ρ the relationships found from the finite element model between the remote loading stress intensity factors, K_I, K_{II} and the local edge stress intensity K_N is given by,

$$\left(\frac{K_N\sqrt{\rho}}{E^*}\right)^3 = 0.9\left(\frac{-K_I}{E^*\rho^{1-\lambda_I}} + 1.09\frac{K_{II}}{E^*\rho^{1-\lambda_{II}}}\right) \quad (4.1)$$

which can be found in Fleury et. al. [19] where there is also a calibration for K_T when the contact size remains constant.

Once these are known it is, in principle, possible to determine the slip zone size, slip displacements and all other relevant quantities using the results in Section 2. Fuller descriptions of this calculation may be found in [19, 20]. There is, however, one provision which was made in relation to this equation, viz. that the contact size remain fixed and, in this context, it should be noted that for general loading trajectories in K_I, K_{II} space the contact size will not remain fixed. This therefore merits much fuller investigation, and our current understanding of this problem will now be presented. Some of the results presented in this article may also be found in Hills and Dini [21] with a greater emphasis on the link between incomplete and complete contacts.

When the plastic zone r_p is small compared to the radius of curvature, ρ , the problem may be considered as two half planes. It is important to know the limits of this assumption. Figure 4.2 shows the loading region where $r_p/\rho < 1$. The stress intensity factors are normalised with ' k ' the yield stress in pure shear. Conversely, when the plastic zone is large compared to the radius of curvature, we may look at the contact as a sharp three quarter plane. Using the mode mixity d_0 as defined in Hills and Dini [22] we quantify the effect of each mode of loading. The contours of d_0/ρ tell us which mode will be dominant when we treat the problem as a three quarter plane.

5 Extended Cattaneo Mindlin Solution

The original partial slip solution devised by Cattaneo [23] and independently discovered by Mindlin [24] is approximate for the axi-symmetric problem they considered (unless the bodies exhibit no Poisson effect) but is exact for plane problems. It hinges on subtracting a shear traction distribution from the sliding distribution with which it is similar and scaled, and rather later Ciavarella and Jäger indepedently noted

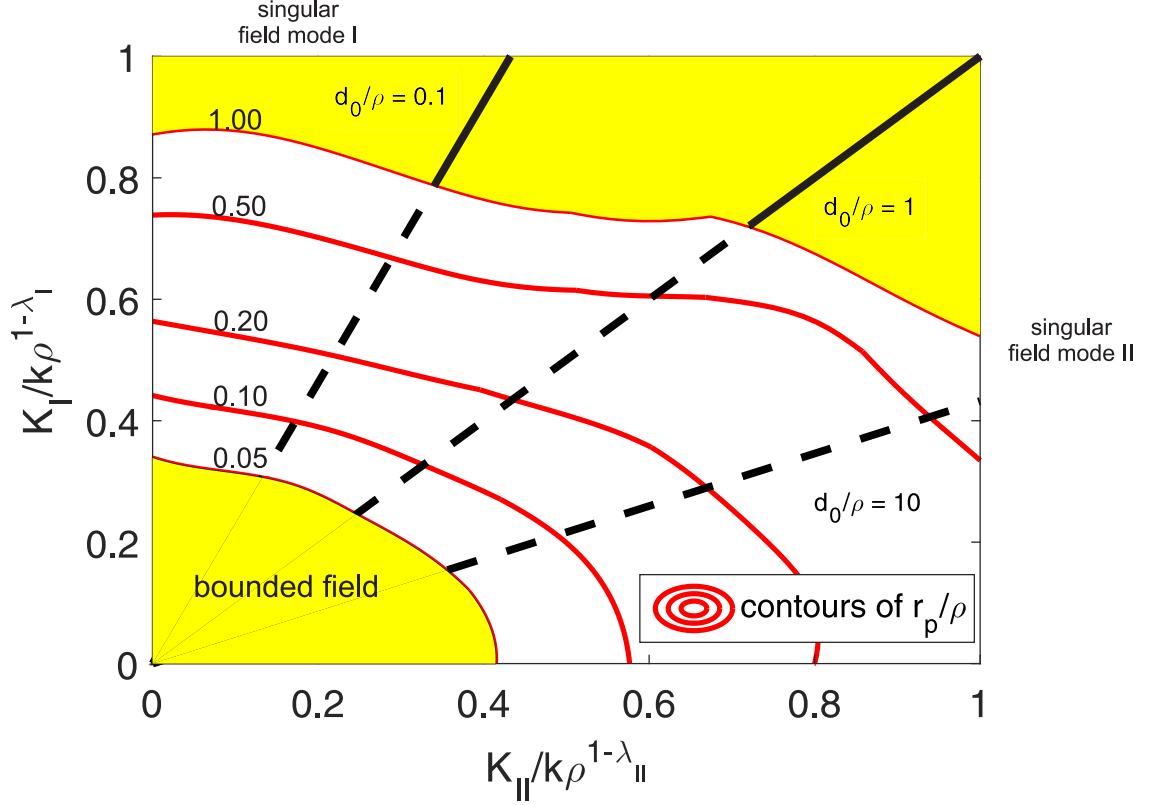
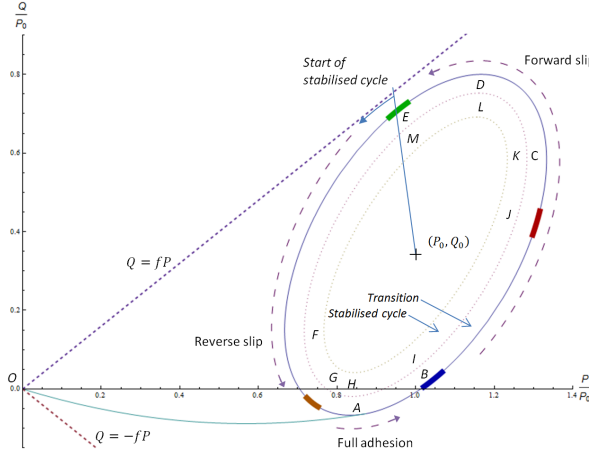
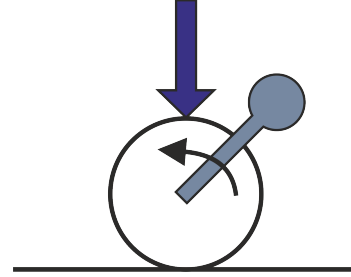


Figure 4.2: Contours of constant r_p/ρ and constant d_0/ρ

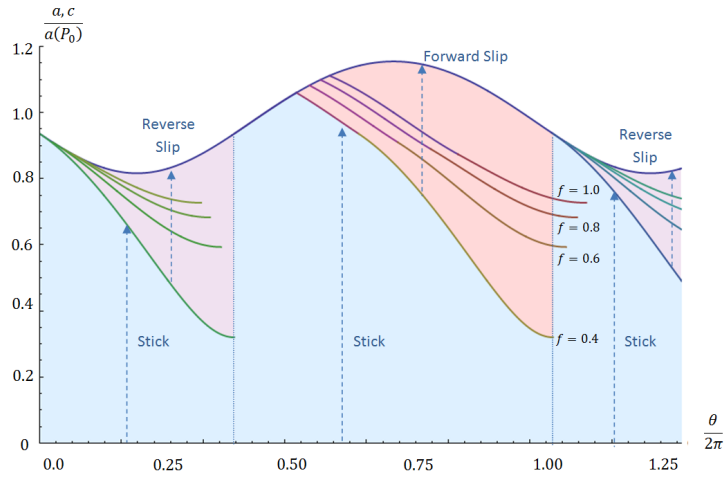
that the same principle might be applied to any contact capable of analysis by half plane methods. The essential feature of these procedures is that, whenever the stick zone is stationary or receding, the differential surface strain acting parallel with the surface, between the contacting bodies, is preserved. In [25, 26] we noted how this same idea may be used, in only a slightly modified form, to any incomplete contact problem (analysed using half-plane procedures), where the interfacial shear traction was induced by a shear force (only) but where the normal load was also permitted to vary. When the change in shear force is such that there is an implied increase in stick zone size in fact it is found that the whole of the contact sticks, and reverse slip, leading, again, to a contracting stick zone ensues. No example has yet been found of a contact problem in this class (incomplete contact) in which the stick zone size increases smoothly - it always either contracts smoothly or the whole contact adheres. The papers cited should be consulted for details, but figures 5.1 show a Hertzian contact subject to a harmonically varying shear force and normal load, with an arbitrary phase shift. The solution (in terms of the extent of slip etc.) is independent of the mean value of the shear force which affects only the locked-in shear.



(a) Loading cycle of contact



(b) Geometry of a Hertzian contact under cyclic loading



(c) Size of contact and slip zones through the loading cycle, a is the contact half-width and c is the stick half-width

Figure 5.1: Hertzian contact with harmonically varying shear force and normal load [26]

An important feature of the solution is that there is a central region within the contact which is permanently adhered. On either side of this is a region which is permanently in contact and which experiences reversing shear (as in a Cattaneo contact). And finally, outside these regions are another pair which periodically include the contact and which experiences unidirectional slip - the material recovers when there is separation, preserving continuity of material.

5.1 Contribution from Asymptotes

A limitation of using the standard procedure introduced above is that it will work only when the slip zones at each contact edge are of the same sign. There will be many combinations of load, where tension is also applied, when this does not hold

and on these occasions the asymptotic solutions introduced near the beginning of this article are very valuable, as we may examine each contact edge in isolation. The extra complication over and above the procedure described in section 2 is that, when the normal load changes, the position of the contact edge changes, and this needs to be taken into account.

First, we re-evaluate the ‘no-bulk-tension’ case in the form of asymptotes. A loading trajectory is followed which maintains full stick, i.e. $\frac{d|Q|}{dP} < f$, and we see that the shearing traction at the end of this loading phase, adjacent to the contact edge $x \rightarrow -a^+$, is

$$q(s) = \int_0^P \left[\frac{\partial K_N}{\partial P} \sqrt{x+a(P)} + \frac{K_N(P)}{2} \frac{1}{\sqrt{x+a(P)}} \frac{\partial a}{\partial P} \right] \frac{dQ}{dP} dP. \quad (5.1)$$

Under these conditions the shear traction is itself square root bounded in form as the contact edge is approached, and we may write

$$q(x+a) \equiv q(s) = K_Q \sqrt{s}. \quad (5.2)$$

This provides us with a one-term approximation to the form of the shearing traction distribution ‘locked in’ during this phase of loading. This point is denoted ‘A’ in Figure 5.2. We now consider what happens when we move to a second phase of loading where the segment in Q-P space exceeds the gradient of the friction cone, and so enter a partial slip regime; three possible trajectories are shown corresponding to receding (AB_3), stationary (AB_2) or advancing (AB_1) contact. The corrective shear traction is found from the Ciavarella-Jäger theorem, which, for a stationary contact, gives

$$\Delta q_{AB_2}(x) = [fK_N(P_B) - K_Q(P_A)] \left(\sqrt{s_B} - \sqrt{s_B - d} \right) \quad (5.3)$$

where the size of the slip zone, d , is here given by

$$d = \frac{2K_T(P_B)}{fK_N(P_B) - K_Q(P_A)}. \quad (5.4)$$

On the other hand, if the contact is advancing we find that

$$\Delta q_{AB_1}(x) = [fK_N(P_B) - K_Q(P_A)] \left(\sqrt{s_B} - \sqrt{s_B - d} \right) + K_Q(P_A) \frac{\Delta a}{2\sqrt{s_B}} \quad (5.5)$$

and where the size of the slip zone, d , is now given by

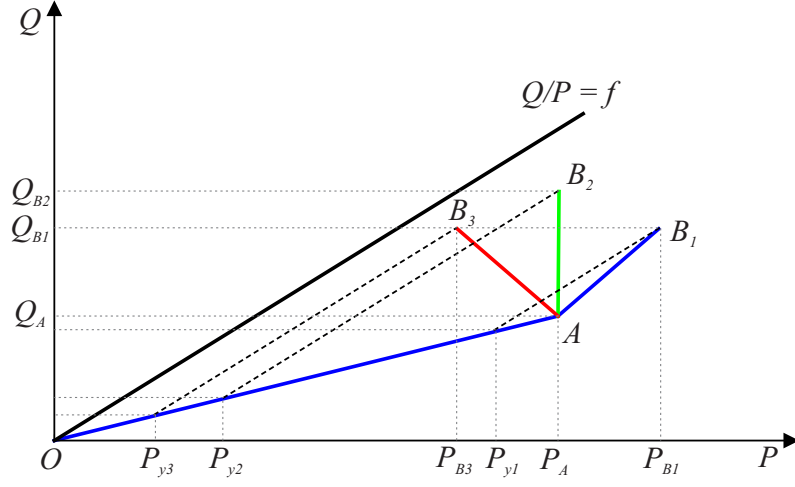


Figure 5.2: Loading paths, stationary contact size (green); advancing contact size (blue) and receding contact size (red)

$$d = \frac{2K_T(P_B) - K_Q(P_A)\Delta a}{fK_N(P_B) - K_Q(P_A)}, \quad (5.6)$$

Example results are shown in Figure 5.3.

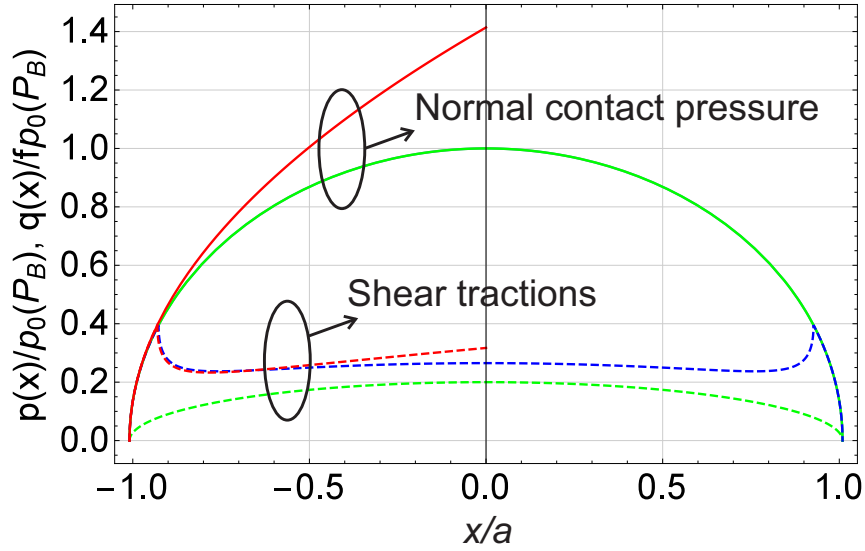


Figure 5.3: Asymptotic approximation for constant contact size. Standard formulation tractions at point A (green); at point B (blue); and asymptotes at point B (red)

6 Receding Contacts

The simplest possible receding contact is shown in Figure 6.1 which depicts a layer pressed onto an elastically similar half plane, first by a normal force, P . It may be shown [27] that this causes the contact to ‘snap’ (under an infinitesimal normal force) to a finite sized contact (here with a half width of about $1.7c$, where c is the layer thickness) although the exact value depends on the friction coefficient, here taken as 0.4. Increases in the normal load do not cause the contact width to change, although both stresses and displacements increase in proportion to the load [28]. Note that there is a central stick zone and two edge slip zones of opposite sign.

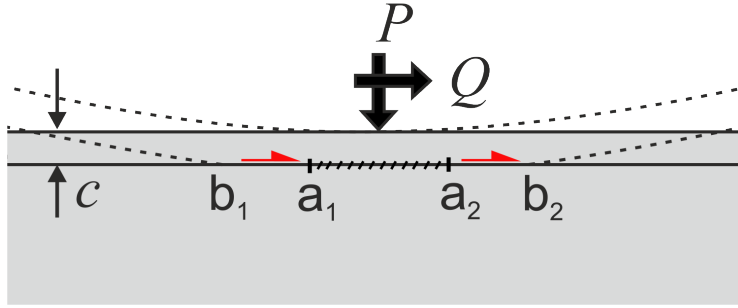


Figure 6.1: Receding contact geometry with slip and stick zones under normal and shear loading

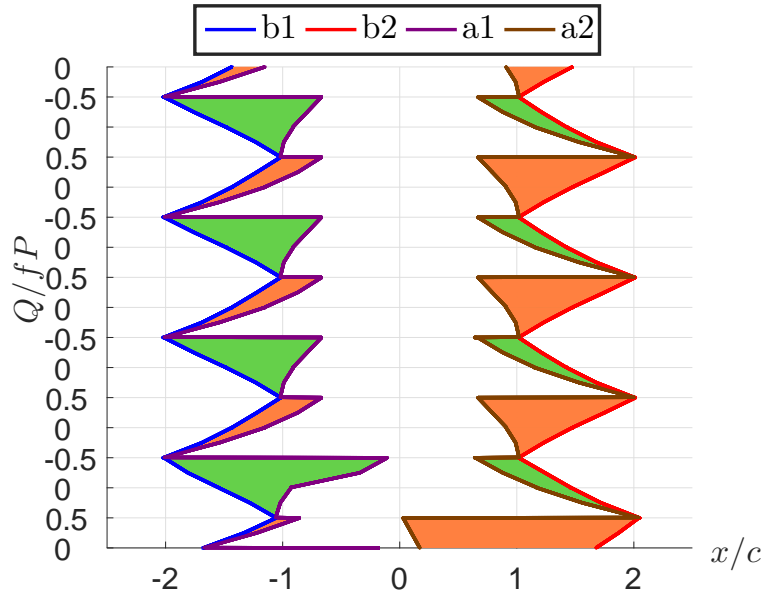


Figure 6.2: Slip displacements for a receding contact under alternating shear loading ($f = 0.4$, $Q_{max}/fP = 0.5$)

We now apply a periodically varying tangential force of magnitude Q , and choose $Q_{max}/fP = 0.5$. This has a very unusual effect. It causes the contact to move, quite significantly (see Figure 6.2) and, at the same time, causes slip zones of the same sign to develop at each edge of the contact patch. The evolution of the traction distribution with time is shown in Figure 6.3. We note that, as expected, the contact patch moves and the slip zone shifts. Also, the contact pressure falls smoothly to zero at the edges so that the contact behaviour resembles a Hertzian (or other incomplete) contact with harmonically varying normal force, as described earlier. It follows that it should be possible to use the asymptotes to describe the evolution of stick and slip history, and hence to use a unified theory to represent their stick slip behaviour.

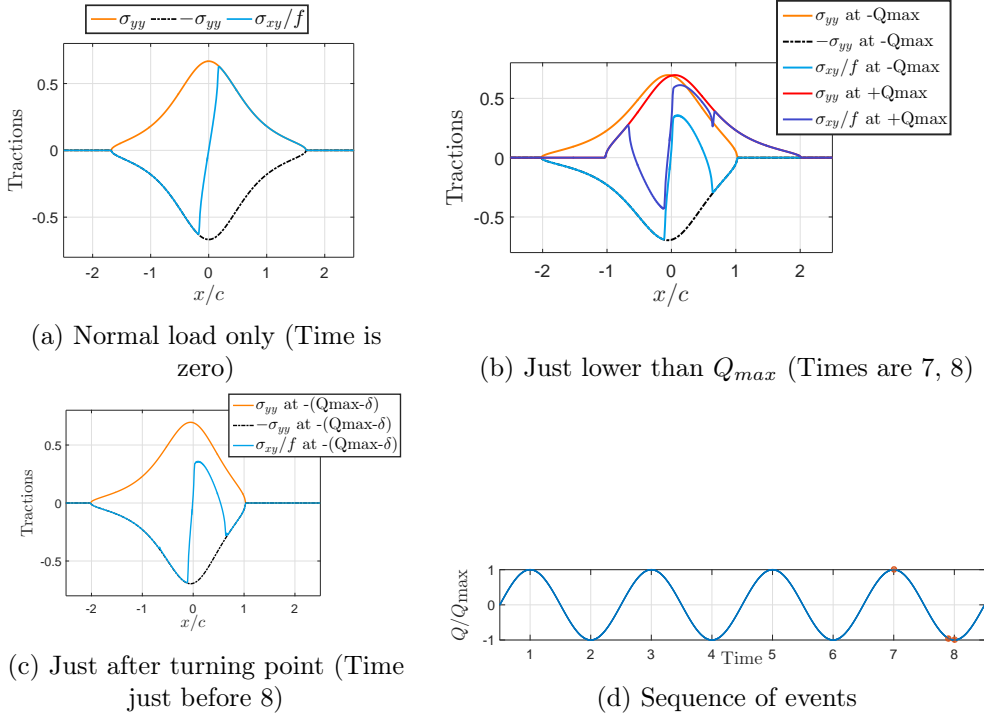


Figure 6.3: Contact tractions for a receding contact under alternating shear loading ($f = 0.4$, $Q_{max}/fP = 0.5$)

7 Conclusion

In this brief review we have classified all possible kinds of contact which may be encountered when the materials in contact are (for example) alloys or ceramics - this would not be exhaustive if the bodies were highly compliant. If we exclude, specifically, complete and common edge contacts we see that the remaining kinds (incomplete non-conformal, incomplete-conformal and receding) may have their contact edge behaviour

described by a very small set of asymptotic forms based on half-plane theory. This very powerful result shows the potential of using laboratory tests conducted using (say) Hertzian contacts for predicting the fretting fatigue behaviour of very different kinds of contact - for example those found under bolted joints. Some aspects of this work (those relating to conformal contacts, contacts with varying normal load and receding contacts) are the subjects of continuing study, and only a synopsis of progress is provided here.

References

- [1] D. A. Hills, D. Nowell, and A. Sackfield. *Mechanics of Elastic Contacts*. Butterworth Heinemann, Jordan Hill, Oxford, 1993.
- [2] C.M. Churchman and D.A. Hills. General results for complete contacts subject to oscillatory shear. *J. Mech. Phys. Solids*, 54(6):1186–1205, 2006.
- [3] C.M. Churchman and D.A. Hills. Slip zone length at the edge of a complete contact. *Int Jnl Solids Struct.*, 43:2037–2049, 2006.
- [4] D.A. Hills and D. Dini. Common edge contacts: Effect of interface line orientation. *International Journal of Mechanical Sciences*, 81(0):73 – 76, 2014.
- [5] R. Ramesh and D. A. Hills. The condition for first slip in a common edge contact subject to in-plane & anti-plane loading. *Jnl. Strain Analysis*, 50(6):386 – 390, 2015.
- [6] M. C. Montebello. *Analysis of the stress gradient effect in Fretting-Fatigue through a description based on nonlocal intensity factors*. PhD thesis, Université Paris-Saclay, 2015.
- [7] M. Ciavarella. The generalized Cattaneo partial slip plane contact problem. i—theory. *Int. J. Solids Struct.*, 35(18):2349 – 2362, 1998.
- [8] J. Jäger. Half-planes without coupling under contact loading. *Arch. Appl. Mech.*, 67:247 – 259, 1997.
- [9] D. Dini and D. A. Hills. Bounded asymptotic solutions for incomplete contacts in partial slip. *Int. J. Solids Struct.*, 41:7049 – 7062, 2004.
- [10] D. Dini, A. Sackfield, and D. A. Hills. Comprehensive bounded asymptotic solutions for incomplete contacts in partial slip. *J. Mech. Phys. Solids*, 53(2):437 – 454, 2005.

- [11] D. A. Hills, R. M. N Fleury, and D. Dini. Partial slip incomplete contacts under constant normal load and subject to periodic loading. *Int. J. Mech. Sci.*, 108-109:115 – 121, 2016.
- [12] A. E. B Mugadu. *Studies in fretting fatigue of complete contacts*. PhD thesis, University of Oxford, 2002.
- [13] N. Banerjee. *The characterisation of fretting fatigue in gas turbine engines*. PhD thesis, University of Oxford, 2010.
- [14] D. A. Hills, A. Thaitirarot, J. R. Barber, and D. Dini. Correlation of fretting fatigue experimental results using an asymptotic approach. *Int. J. Fatigue.*, 43:62 – 75, 2012.
- [15] D. Nowell. *An analysis of fretting fatigue*. PhD thesis, University of Oxford, 1988.
- [16] M. P. Szolwinski and T. N. Farris. Observation, analysis and prediction of fretting fatigue in 2024-t351 aluminum alloy. *Wear*, 221(1):24 – 36, 1998.
- [17] L. Bertini and C. Santus. Fretting fatigue tests on shrink-fit specimens and investigations into the strength enhancement induced by deep rolling. *Int. J. Fatigue*, 81:179 – 190, 2015.
- [18] A. Mugadu, D. A. Hills, J. R. Barber, and A. Sackfield. The application of asymptotic solutions to characterising the process zone in almost complete frictional contacts. *Int. J. Solids Struct.*, 41:385 – 397, 2004.
- [19] R. M. N. Fleury, D. A. Hills, and J. R. Barber. A corrective solution for finding the effects of edge rounding on complete contact between elastically similar bodies. part i: Contact law and normal contact considerations. *Int. Jnl. Solids and Structures*, 85 - 86:89 – 96, 2016.
- [20] R. M. N. Fleury, D. A. Hills, and J. R. Barber. A corrective solution for finding the effects of edge rounding on complete contact between elastically similar bodies. part ii:near-edge asymptotes and the effect of shear. *Int. Jnl. Solids and Structures*, 85-86:97 – 104, 2016.
- [21] D. A. Hills and D. Dini. A review of the use of the asymptotic framework for quantification of fretting fatigue. *J. Strain Analysis*, 51(4):240 – 246, 2016.
- [22] D.A. Hills and D. Dini. Characteristics of the process zone at sharp notch roots. *Int. J. Solids and Struct.*, 48(14-15):2177–2183, 2011.

- [23] C. Cattaneo. Sul contatto di due corpi elastici. *Atti Accad. naz. Lincei Rc*, 27:342–348, 434–436, 474–478, 1938.
- [24] R. D. Mindlin. Compliance of elastic bodies in contact. *J. Appl. Mech. Trans. ASME*, 16:249 – 268, 1949.
- [25] D. A. Hills, M. Davies, and J. R. Barber. An incremental formulation for half-plane contact problems subject to varying normal load, shear and tension. *J. Strain Analysis*, 46(6):436 – 443, 2011.
- [26] M. Davies, J. R. Barber, and D. A. Hills. Energy dissipation in a frictional incomplete contact with varying normal load. *Int. J. Mech. Sci.*, 55(1):13 – 21, 2012.
- [27] T. Chaise, R. J. H. Paynter, and D. A. Hills. Contact analysis of a semi-infinite strip pressed into a half plane by a line force. *Int. J. Mech. Sci.*, 81:60 – 64, 2014.
- [28] M.E. Kartal, J.R. Barber, D. A. Hills, and D. Nowell. Partial slip problem for two semi-infinite strips in contact. *Int. J. Eng. Sci.*, 49:203–211, 2011.